ULTRASOUND NEWS

3-2026

The role of transabdominal ultrasound in pancreatic cyst surveillance: correlation with cross-sectional imaging findings and malignancy risk

ULTRA SONO GRAPHY

ORIGINAL ARTICLE

Sun Kyung Jeon[1], Jung Hoon Kim[1,2], Hyo-Jin Kang[1]

[1]Department of Radiology, Seoul National University Hospital, Seoul National University College of Medicine, Seoul; [2]Institute of Radiation Medicine, Seoul National University Medical Research Center, Seoul National University Hospital, Seoul, Korea

https://doi.org/10.14366/usg.25193
eISSN: 2288-5943
Ultrasonography 2026;45:174-183

Received: September 23, 2025
Revised: December 5, 2025
Accepted: January 5, 2026

Correspondence to:
Jung Hoon Kim, MD, Department of Radiology, Seoul National University Hospital, Seoul National University College of Medicine, 101 Daehak-ro, Jongno-gu, Seoul 03080, Korea
Tel. +82-2-2072-3107
Fax. +82-2-743-6385
E-mail: jhkim2010@snu.ac.kr

Purpose: This study aimed to evaluate the clinical utility of transabdominal ultrasound (TAUS) for pancreatic cyst surveillance by assessing its concordance with follow-up computed tomography (CT) and magnetic resonance imaging (MRI) findings and the associated risk of malignancy.

Methods: This retrospective study included 523 patients who underwent TAUS for pancreatic cysts (≥1 cm), followed by contrast-enhanced CT or MRI within a 1-year interval between 2021 and 2022. Cysts were classified as high-risk if they exhibited any high-risk stigmata or worrisome features, and as low-risk otherwise, based on the 2024 international consensus guidelines. TAUS classifications were compared with those from CT/MRI. In a subset of 164 patients with reference standards, malignancy rates were compared between high- and low-risk cysts on TAUS.

Results: The overall cyst identification rate on TAUS was 88.7% (464/523), with identification rates higher in patients with lower body mass index (23.8±3.3 kg/m^2 vs. 29.2±3.3 kg/m^2, P=0.003) and in those with non-tail cyst locations (92.7% [406/438] vs. 68.2% [58/85] for tail lesions, P<0.001). Among identified cysts, 86 (18.5%) were classified as high-risk and 378 (81.5%) as low-risk. TAUS-based risk classification demonstrated significant correlation with CT/MRI classification (P<0.001). The likelihood of a high-risk cyst on CT/MRI increased with the number of high-risk or worrisome features identified on TAUS. Malignancy rates were significantly higher in high-risk cysts than in low-risk cysts based on TAUS assessment (12.5% [4/32] vs. 1.5% [2/132], P=0.014).

Conclusion: TAUS may serve as a useful noninvasive imaging modality for pancreatic cyst surveillance, particularly in patients with favorable visualization conditions. TAUS features correlated well with CT/MRI findings in identifying high-risk pancreatic cysts, and the presence of multiple worrisome features on TAUS was associated with an increased likelihood of high-risk classification on subsequent cross-sectional imaging.

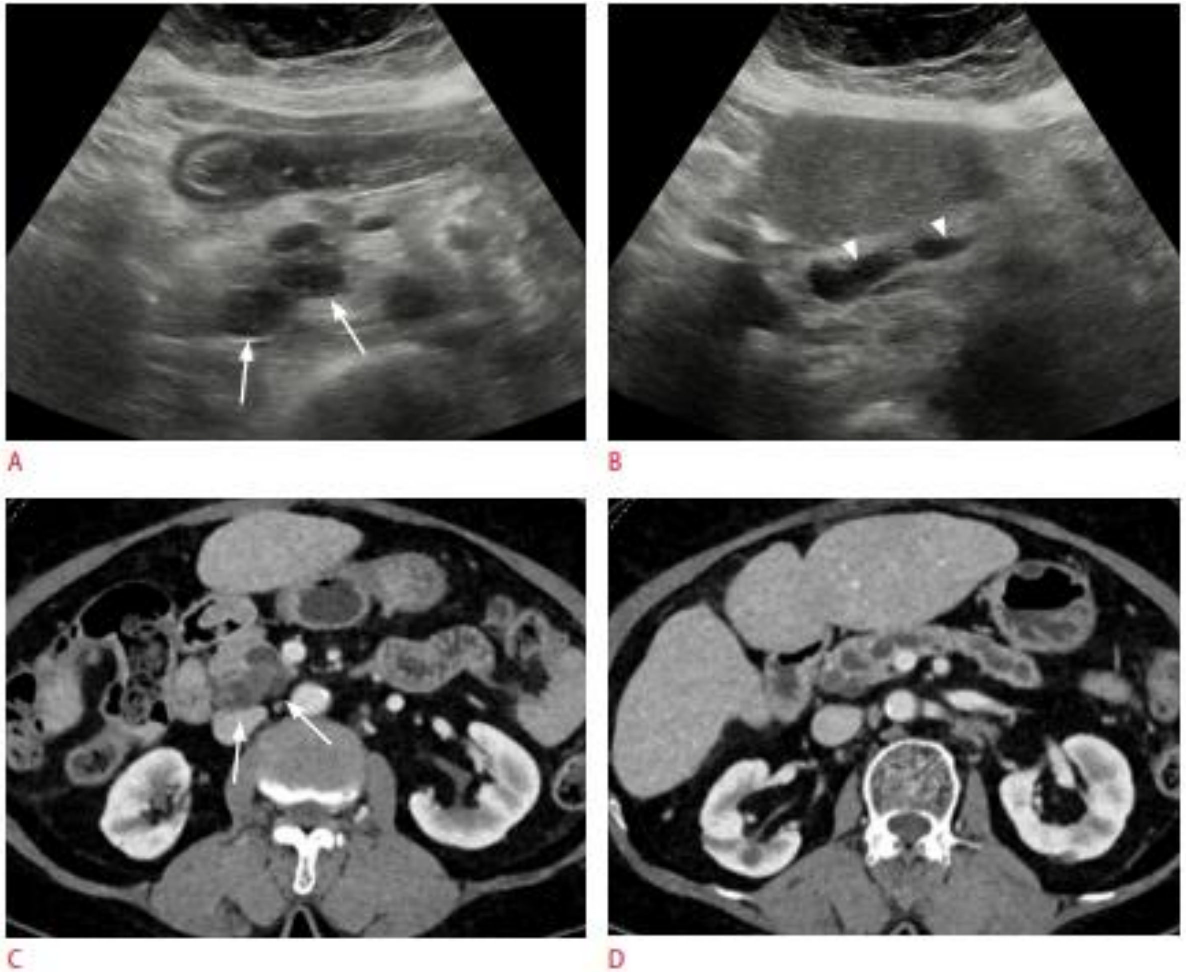

Fig. 3. An 83-year-old female patient who underwent transabdominal ultrasound (TAUS) (A, B) and follow-up contrast-enhanced computed tomography (CT) (C, D) for a pancreatic uncinate process cyst.
A, B. TAUS reveals a 3.6 cm cystic lesion (arrows) in the pancreatic uncinate process with a thickened septum and main pancreatic duct (MPD) dilatation of 8 mm (arrowheads), suggestive of a high-risk cyst. C, D. Contrast-enhanced CT demonstrates a corresponding 3.8 cm cystic lesion (arrows) in the pancreatic uncinate process with MPD dilatation of 8 mm, consistent with high-risk classification.

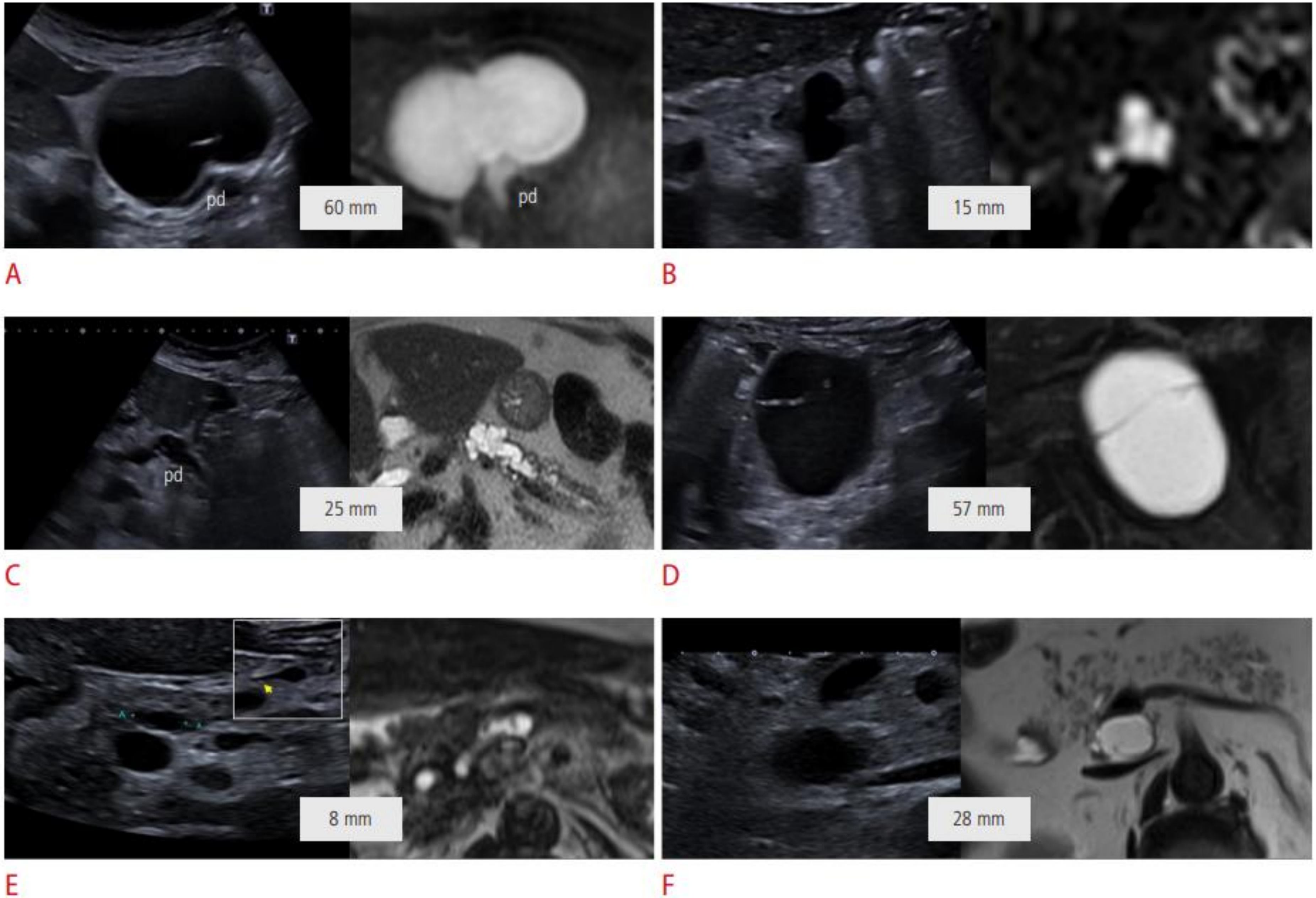

Fig. 4. Correlative imaging between targeted abdominal ultrasound (TAUS) and magnetic resonance imaging (MRI) in various pancreatic cystic lesions.

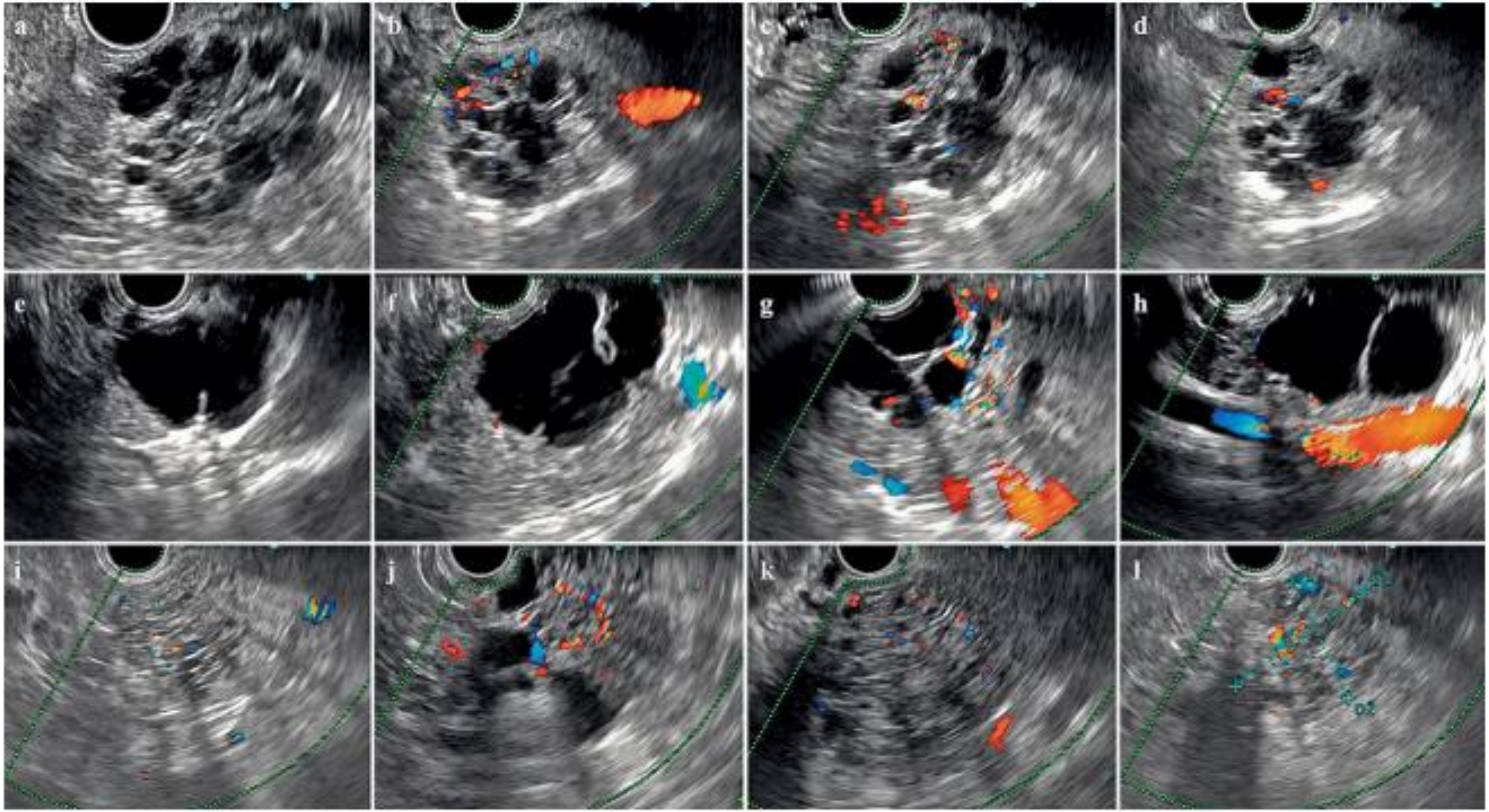

Fig 4. EUS manifestations of SCN subtypes. Panels a-d demonstrated microcystic type. Panels e-h illustrated macro-cystic type.

WFUMB Ultrasound Open 3 (2025) 100080

Contents lists available at ScienceDirect

WFUMB Ultrasound Open

journal homepage: www.journals.elsevier.com/wfumb-ultrasound-open

Original Contribution

Treatment of inoperable pancreatic adenocarcinoma with focused ultrasound and microbubbles in patients receiving chemotherapy

Margrete Haram [a,b,c], Rune Hansen [d,e], Ola Finneng Myhre [e], Stian Solberg [f], Naseh Amini [f], Bjørn Atle Angelsen [f], Catharina de Lange Davies [g,*], Eva Hofsli [b,c]

[a] Department of Radiology and Nuclear Medicine, St. Olav's Hospital - Trondheim University Hospital, Norway
[b] Department of Clinical and Molecular Medicine, Norwegian University of Science and Technology, Norway
[c] Cancer Clinic, St. Olav's Hospital - Trondheim University Hospital, Norway
[d] Department of Health Research, SINTEF Digital, Trondheim, Norway
[e] Department of Circulation and Medical Imaging, Norwegian University of Science and Technology, Norway
[f] SURF Technology AS, Trondheim, Norway
[g] Department of Physics, Norwegian University of Science and Technology, Norway

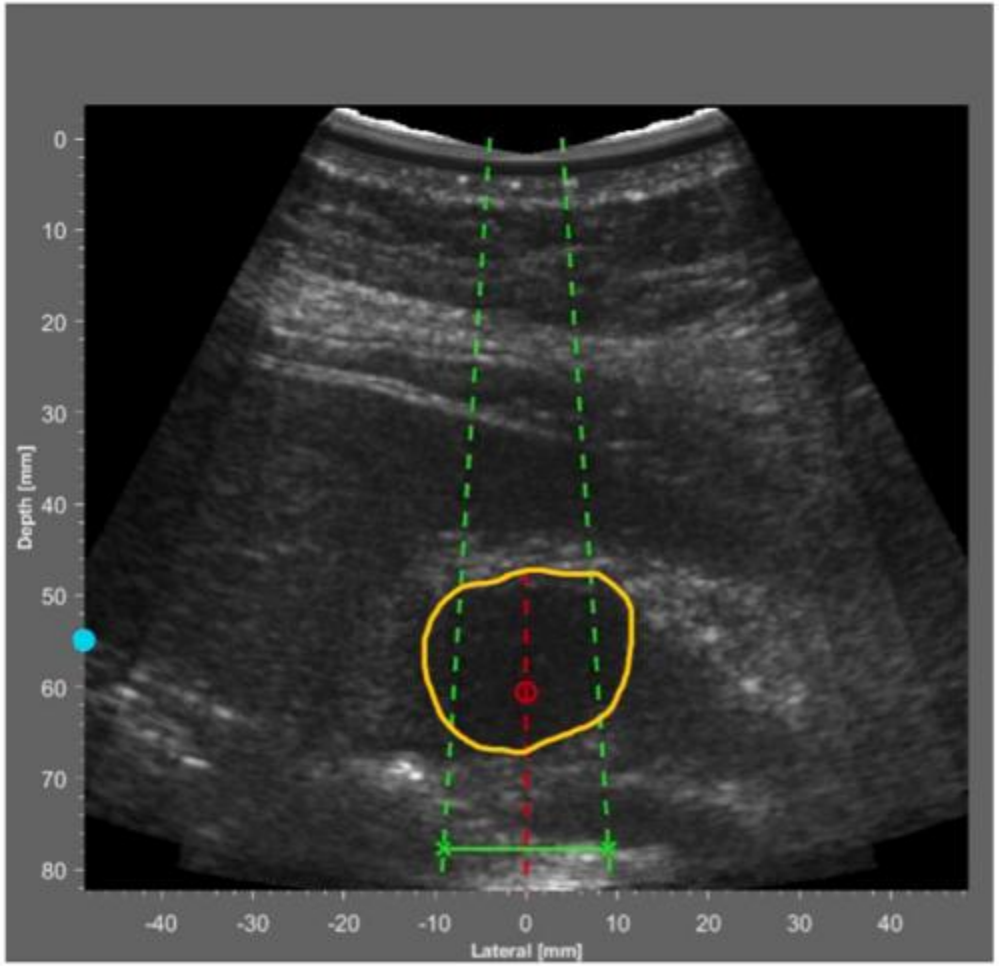

Fig. 3. Adjustment of therapy beams. Green dashed lines: center axis of individual therapy beams. The number and spacing between therapy beams were chosen to cover the entire tumor without significant overlap between the beams. Green horizontal line: geometric focus depth of the therapy beams. Yellow line: tumor. Red circle: depth of maximum derated LF MI as measured in a water tank. Dashed red line: depth region where the LF MI is within −1 dB of said maximum. Cyan circle: the geometric focus of HF beams.

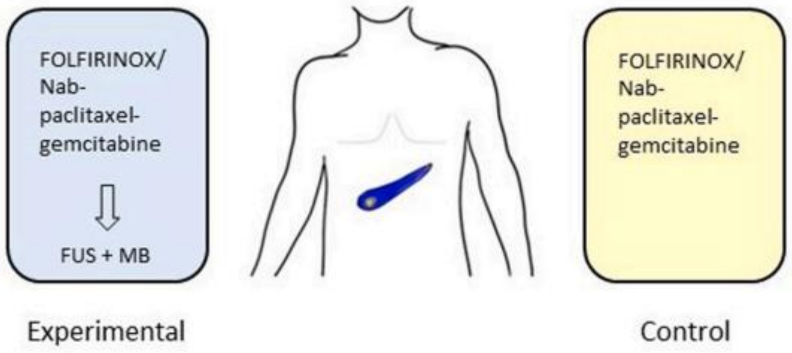

Fig. 1. Randomization 1:1. Experimental arm to the left (blue) receiving chemotherapy (FOLFIRINOX or nab-paclitaxel-gemcitabine) combined with FUS + MBs. Control arm to the right (yellow) receiving chemotherapy only.

Fig. 2. Timeline of experimental treatment. Chemotherapy, that is, FOLFIRINOX or gemcitabine-nab-paclitaxel, is administered sequentially. FUS + MBs were administered as soon as possible after the completed infusion on day one. Boluses of Sonovue were given every 3.5 min and repeated nine times. In the case of FOLFIRINOX, the 46h infusion of fluorouracil was started immediately after completed FUS + MB treatment.

The value of Ultrasound Fat Fraction as compared to Controlled Attenuation Parameter for the severity of liver steatosis assessment - preliminary results

Camelia Nica, Ioan Sporea, Alexandru Popa, Raluca Lupușoru, Maria Voicu Stan Erimescu, Roxana Șirli, Mirela Dănilă, Daiana Boleac, Ariadna Plesa, Alina Popescu

Abstract

Aim: Liver steatosis is a growing global health concern with significant medical and economic implications. This study aimed to evaluate USFF (ultrasound fat fraction) for steatosis assessment as compared to controlled attenuation parameter (CAP).

Materials and methods: Liver steatosis was assessed in the same session by QUS (Samsung Medison RS85) and CAP (FibroScan Compact M530) in a cohort of 169 patients. For QUS, TAI and TSI measurements were acquired, then Fat Fraction (%) was calculated and displayed. The CAP cut-off values for S1, S2 and S3 were 248, 268 and 280 dB/m, respectively. ROC analysis was performed to identify the best cut-off values for USFF for each steatosis stage.

Results: Of the 169 patients, 52.6% had at least moderate steatosis by CAP. Moderate correlations were observed for TSI vs. CAP (r=0.66), TAI vs. CAP (r=0.83), and TSI vs. TAI (r=0.68), with good diagnostic performance (TSI AUROC=0.82, TAI AUROC=0.81). A strong correlation between USFF and CAP was also found (r=0.81, p<0.001). The best USFF cut-off value to identify at least mild steatosis in all patients was >5% with very good performance (AUROC=0.90) for moderate steatosis the cut-off value was >7.5% (AUROC=0.92) and for severe steatosis, >10% (AUROC=0.91).

Conclusion: USFF seems to be a promising tool for diagnosing liver steatosis, with a very good performance.

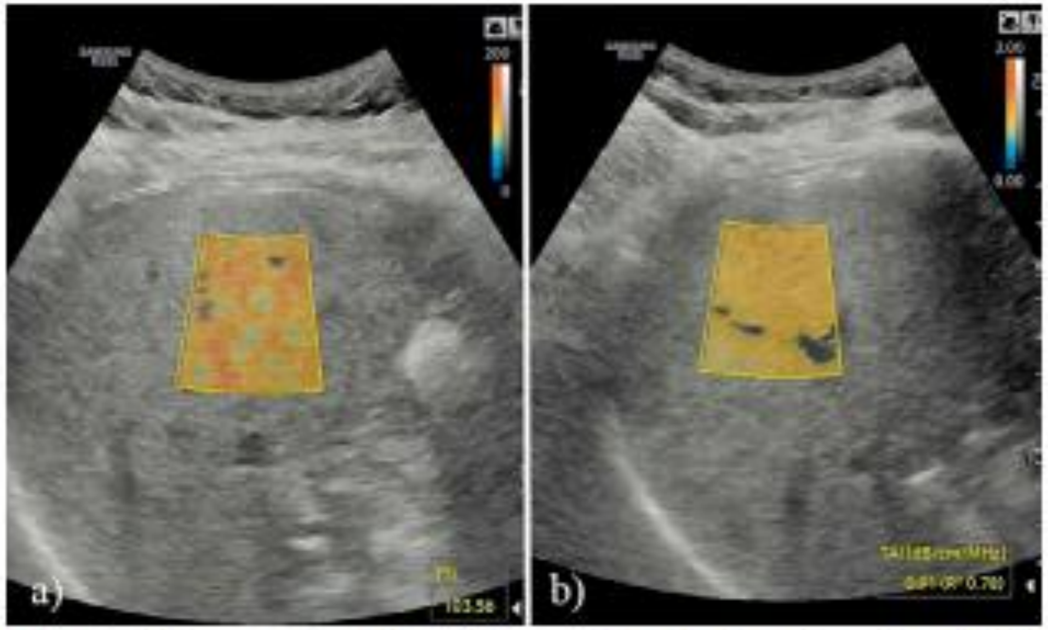

Fig 1. a) Parametric Tissue Scatter-distribution Imaging (TSI) map of the liver obtained on the Samsung RS85 device. A 2×3 cm ROI (region of interest) with a color-coded map was generated, overlaid on the B-mode image, positioned at least 2 cm below the liver capsule. On the right inferior corner, the value of TSI is displayed; b) Parametric Tissue Attenuation Imaging (TAI) map of the liver obtained on the Samsung RS85 device. A 2×3 cm ROI (region of interest) with a color-coded map was generated, overlaid on the B-mode image, positioned at least 2 cm below the liver capsule. On the right inferior corner, the value of TAI is displayed in db/cm/MHz and and the quality parameter R^2.

Fig 2. Automated quantitative ultrasound report for hepatic fat assessment (Samsung RS85 system). The figure illustrates the system-generated QUS report obtained from the hepatic region of interest. The display shows the measured parameters: TAI (Tissue Attenuation Imaging), TSI (Tissue Scatter-distribution Imaging), and the automatically derived USFF (Ultrasound Fat Fraction), which provides a quantitative estimate of hepatic steatosis. Each parameter is reported with its mean and median values, accompanied by a quality index that reflects measurement stability and reliability. The USFF value is automatically calculated by the ultrasound system's embedded algorithm based on the attenuation and backscatter coefficients (TAI and TSI). No manual post-processing was performed by the operator.

Ultrasound characteristics of early glottic laryngeal cancer: diagnostic value and preoperative T staging

Hua Wang, Lei Sun, Xiang-ru Wang, Xin-xin Lu, Fang-xi Zhao, Si-yuan Zhang, Liang Wu, Xiao-peng Li

Abstract

Aim: To analyze the ultrasound characteristics of early glottic laryngeal cancer and evaluate their value in diagnosis and T-stage prediction.

Material and methods: A total of 154 patients with postoperative diagnosis of early glottic cancer were included. Ultrasonic findings were summarized, and factors influencing diagnosis and T staging were analyzed.

Results: Key findings included mucosal roughness, reduced echogenicity, vocal cord masses, and Adler grade III blood flow. Ultrasound showed 87.66% sensitivity. Adler grade and vocal cord mass were independent predictors of diagnosis. T-staging concordance was 74.51% for T1a, 72.73% for T1b, and 86.21% for T2, with no significant difference among stages. Adler grade and resistance index differed significantly across T stages, with resistance index and vocal cord mass being independent staging factors.

Conclusion: Ultrasound can clearly distinguish mucosal layer lesions on the vocal cords, and it has a certain value in the diagnosis and T staging of early glottic laryngeal cancer.

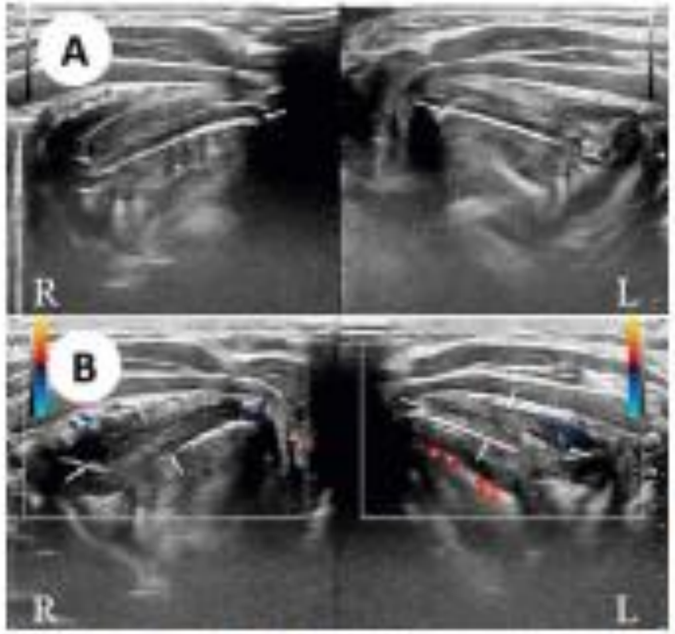

Fig 2. Normal vocal cord ultrasound images: A) The normal mucosal layer of the vocal cords is a continuous and smooth hyperechoic band, while Normal vocal cords exhibit low echogenicity; B) Normal vocal cords only show a few punctate blood flow signals, Alder grade I.

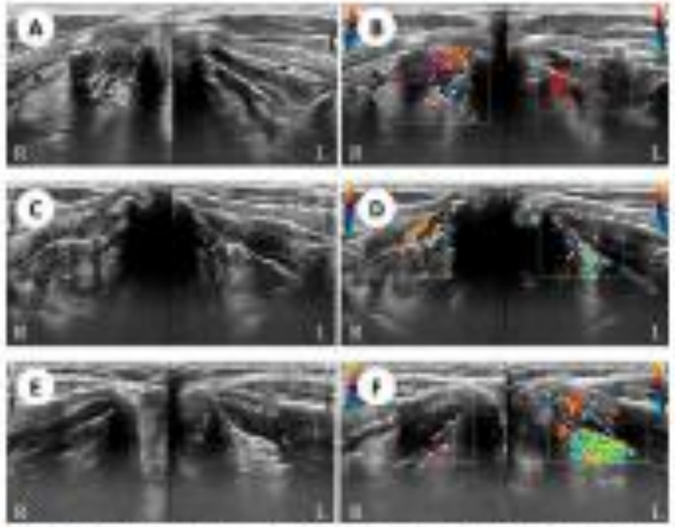

Fig 3. Ultrasound imaging features of T1- and T2-stage laryngeal cancer: A) Male, 49 years, with hoarse voice for 2 months, postoperatively diagnosed with T1a stage cancer. The right vocal cord mucosa (arrow) appears rough with discontinuous echogenicity, and a hypoechoic mass can be seen at the front; B) CDFI evidences a rich and chaotic blood supply within the mass, with visible thickened and tortuous blood vessels (Adler grade III); C) Male, 61 years, with hoarse voice for 7 months, postoperatively diagnosed with T1b stage cancer. Both vocal cord mucosae appear rough with discontinuous echogenicity (arrow), and hypoechoic masses can be seen in the anterior and middle parts of both vocal cords. The mass on the left vocal cord invades the superficial muscle layer; D) CDFI reveals a rich and chaotic blood supply within the mass (arrow), with visibly thickened and tortuous blood vessels (Adler grade III). The rich blood supply area of the left vocal cord appears only in the superficial muscle layer; (E) Male, 57 years, with hoarse voice for 6 months, postoperatively diagnosed with T2 stage cancer. The left vocal cord mucosa appears rough with discontinuous echogenicity (arrow), and a hypoechoic mass is visible throughout the entire length of the vocal cord, extending upward and downward but not in the paraglottic space. The right vocal cord mucosa appears smooth; F) CDFI shows a rich and chaotic blood supply within the mass (arrow), with visible thickened and tortuous blood vessel (Adler grade III).

Why is ultrasound needed in inflammatory bowel disease?

Frauke Petersen[1], Michael Höpfner[2], Christian Jenssen[3], Dieter Nürnberg[4], Deike Strobel[5], Johanna Vogelpohl[6], Christoph F Dietrich[7]

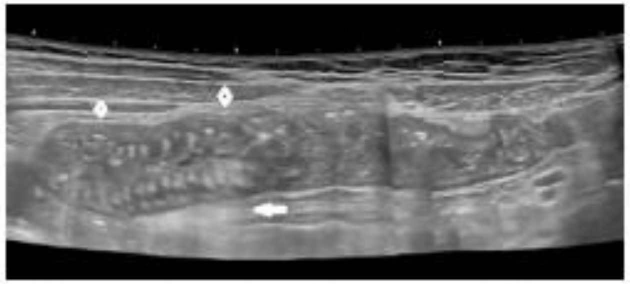

Fig 1. Crohn's disease, special aspect of involvement of the proximal jejunum. Linear probe 9 MHz, panoramic-view-technique in the mid-abdomen demonstrating the sudden appearance of swollen circular folds in the marked region, mesenteric fatty proliferation underneath discreet (arrow). Finding verified by upper enteroscopy and biopsy.

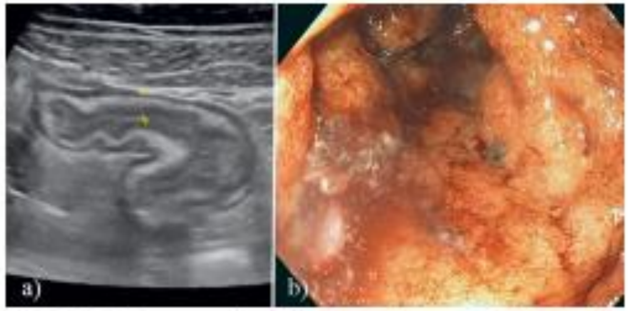

Fig 2. Left lower quadrant, horizontal plane, 9 MHz probe. Typical aspect of an acute flare of UC, 4.3 mm wall thickness, inner hypoechoic layer prominent (mucosa). The lumen is almost empty, the curved aspect indicating a preserved elasticity of the colon. Corresponding endoscopic finding: Mayo score 3.

Abstract

Intestinal ultrasound had been performed in several countries for more than 30 years, but for a longer period had been in the hands of few experts. With new evidence showing that the method is accurate and has excellent performance especially in treatment monitoring and detection of complications of IBD, there is a growing interest in performing this method by those physicians who care for IBD patients in in- and outpatient settings. The authors are convinced that intestinal ultrasound is helping to reduce radiation exposure and enables fast and less expensive decision-making by taking patients' needs into account. This paper series contains three parts. This first part summarizes guideline recommendations on the use of ultrasound in IBD, describes the typical findings that can be obtained at the point of care without advanced ultrasound technologies and helps to standardize documentation. The second part will provide an overview on actual ultrasound-activity-scores in IBD and report about advanced multimodal ultrasound modalities and endoscopic and interventional ultrasound. These modalities should be provided by specialized IBD centers. The third part will enhance a wider overview of treatment control, mural and extramural disease complications as well as extraintestinal manifestations. Advantages and limitations of the method are discussed, with an outlook how to optimize implementation in the future.

Keywords: gastrointestinal tract; ultrasound; Magnetic Resonance Imaging; computed tomography; endosonography

Table II. Recommendation for standardised reporting of US findings in IBD (developed on basis of the German consensus recommendations [21] and a proposal of Japanese authors [57]).

Standardised reporting
Indication
Relevant information from the patient's medical history and current clinical situation
Examination technique
• Specification of the US system and probes used (Type, frequency)
• Specification of the applied US techniques in addition to B-Mode (e.g. Colour Doppler imaging, contrast-enhanced US, oral contrast, elastography)
• Comprehensive gastrointestinal US examination versus focused examination (to be specified)
Imaging quality and limitations
• Examination on fasting patient +/–
• Good imaging quality, no limitations / Limitations (to be described) / Poor quality
Findings assigned to the different parts of the large and small intestine (Rectum, sigmoid colon, descending colon, transverse colon, ascending colon, ileocecal valve, appendix, terminal ileum, Ileum, jejunum, duodenum) and peritoneal cavity
• Maximum BWT: ____mm (facultatively: submucosa thickness, related to BWT [%])
• Stratification: well delineated/blurred/lost
• Haustration (only large intestine): preserved/reduced/lost
• Length of the segments affected
• Vascularity (CDI): normal/increased (Limberg score___)
• Mesenteric wrapping/ i-fat): +/–
• Enlarged peri-intestinal lymph nodes: +/–
• Exudation/ free peritoneal fluid: +/–
• Abscess +/– if +: diameter (___ x ___ mm), accessibility for percutaneous puncture +/–
• Fistula +/– if +: Type, connecting ___ and ____
• Stricture +/– if +: Length (____ mm)
• Motility (Small intestine):reduced/ normal/ increased/ pendulating peristalsis
• Tenderness with the US probe: +/–
• Extraintestinal manifestation, e.g., US signs of PSC
• Additional findings, e.g., free fluid
• Diagnostic or therapeutic US-guided intervention: +/–, if +: description
Documentation (images, video files)
Summary (potentially including US IBD activity score, differential diagnosis) **and clinical conclusion**

BWT – Bowel Wall thickness; CDI – Colour Doppler Imaging.

Fig 3. Left lower quadrant, linear 7 MHz probe. Ulcerative colitis after 8 years of duration. Typical aspect with relatively small mucosal and relatively large hyperechoic submucosa.

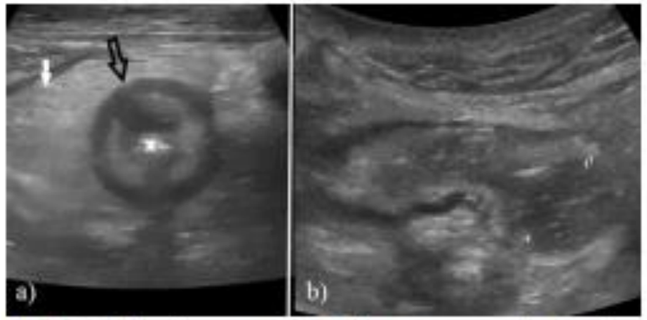

Fig 4. Crohn's disease, terminal ileum, cross-sectional view, 9 MHz linear probe: Thickened intestinal wall with narrowed luminal gas (x), three layers of the bowel wall are visible as a "target sign": exterior hypoechogenic dark layer: muscularis propria, hyperechoic middle layer: submucosa, hypoechoic central layer: mucosa. The stratification of the layer is disturbed in a focal sector (dark arrow), typical for CD. The thickened terminal ileum is embedded in a hyperechoic mass of mesenteric fat ("echogenic wrapping" or "i-fat"white arrow), distancing this part of the bowel from the abdominal wall, as well as from lateral and dorsal muscular structures. Corresponding longitudinal aspect with widening of measured 2,1 cm of the upstream small bowel in the same patient (a,b). The sectoral blurring of the stratification in the cross-sectional image (a) is missed in the longitudinal plane for geometric reasons (b).

Fig 5. Lower abdomen in medial sagittal plane, 9 MHz linear probe. Crohn's disease, fixed loop of a thickened preterminal ileum, adherent to the top of the bladder without obvious open fistula.

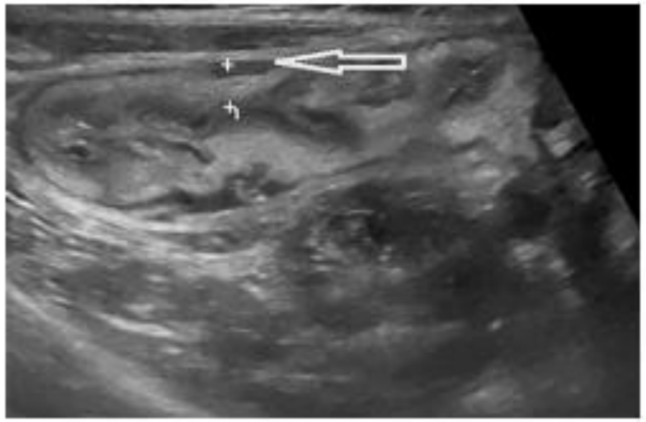

Fig 6. Right lower quadrant, linear probe 9 MHz, cross section of the cecum: right sided ulcerative colitis, acute flare. Demonstrating difficulties in measurement procedures: the luminal air has almost vanished, and the lumen can just be estimated. Folds could be mistaken as thickened wall. As in this case, measuring

able and reproducible parameter for the delimitation of a pathological intestinal wall thickness [13,15, 45-47]. The wall thickness should be measured in a standardized manner at the point of maximum wall thickness, although the exact methodology is disputed among experts. Although guidelines suggest measuring in longitudinal section or using two measurements each in longitudinal and in cross-section, mathematical considerations indicate a higher reproducibility and accuracy of the measurement

Sonopsychology in obstetrics, gynecology, and pediatrics: psychological dimensions of ultrasound practice

Florian Recker, Jessica Leimgruber, Susan Campbell Westerway, Carmel M Moran, Eberhard Merz, Simone Schwarz, Burkhard Möller, Dagmar Schreiber-Dietrich, Christoph Frank Dietrich

Abstract

Ultrasound (US) examinations are not only diagnostic procedures but also psychologically charged experiences that shape patients' perceptions, emotions, and behaviors, a field we term sonopsychology. In obstetrics, US functions as both a clinical and psychosocial milestone: it reassures parents, strengthens maternal-fetal bonding, and provides shared experiences, while simultaneously provoking anxiety, especially in high-risk pregnancies or when abnormal findings are detected. Effective communication, empathetic interaction, and involvement of partners and family are critical in reducing distress and enhancing attachment. In gynecology, US examinations may raise fears related to fertility, chronic disorders, or cancer, with transvaginal studies carrying additional vulnerability due to their intimate nature. Sensitive handling, informed consent, and respectful interaction are therefore essential. Pediatric US presents unique challenges, as cooperation depends on developmental stage, prior experiences, and the emotional climate of the exam. Strategies such as age-appropriate explanations, play, distraction, and parental presence are vital to minimize fear and encourage trust. Across all patient groups, sonopsychology emphasizes that ultrasound is more than imaging; it is a human encounter where communication, empathy, and psychological awareness directly influence outcomes. Future research should refine interventions to reduce "scanxiety," explore child- and family-centered approaches, and optimize the integration of psychological care into routine sonography.

Why sonographers should not lose sleep over AI?

Ahmad J. Abdulsalam

Department of Physical Medicine and Rehabilitation, Mubarak Alkabeer Hospital, Kuwait

The question echoing through musculoskeletal (MSK) ultrasound departments worldwide is no longer "if" artificial intelligence will impact our field, but "how much" and "should we be worried?" After examining the current landscape of AI development in musculoskeletal ultrasound, I believe the answer is clear: we should be excited, not anxious (fig 1).

Unlike other imaging modalities, ultrasound presents distinct challenges that make complete AI automation particularly difficult [1]. The operator-dependent nature of our examinations – requiring real-time decisions about probe positioning, patient interaction, and dynamic assessment – creates a complexity that current AI systems struggle to overcome [2]. When we perform MSK ultrasound, we are not simply capturing static images; we are conducting a dynamic, real-time investigation that integrates clinical context, patient response, and anatomical variability. This inherent complexity, often viewed as a limitation, may actually be our greatest asset in the age

Fig 1. A sonographer losing sleep over AI.

and enhanced visualization through advanced processing algorithms. These tools represent what AI does best –

yêu cầu quyết định ngay lập tức về vị trí đầu dò, tương tác với bệnh nhân và đánh giá động – LÀ một phức tạp mà các hệ thống AI hiện tại khó vượt qua